Unravelling the fabric of the human mind: the brain-cognition space

Valentina Pacella (valentina.pacella.90@gmail.com)
CNRS University of Bordeaux https://orcid.org/0000-0001-6168-9954
Victor Nozais
Institut des Maladies Neurodégénératives-UMR 5293 https://orcid.org/0000-0003-2529-1839
Lia Talozzi
CNRS, University of Bordeaux https://orcid.org/0000-0003-1827-0407
Stephanie J Forkel
Donders Centre for Cognition, Radboud University,
Michel Thiebaut de Schotten
CNRS, University of Bordeaux https://orcid.org/0000-0002-0329-1814

Social Sciences - Article

Keywords:

Posted Date: November 15th, 2022

DOI: https://doi.org/10.21203/rs.3.rs-2260331/v1

Abstract

Thirty years of functional neuroimaging have been accumulating a wealth of evidence of the intricate relationship between structure and function. However, potential overlap, independence, granularity of and gaps between functions remain poorly understood at the global level. In this study, we extracted the latent structure of the current brain-cognition knowledge and revealed its organisational structure. This knowledge has been derived from the most comprehensive meta-analytic fMRI database (Neurosynth) that was used to compute a two-dimensional embedding space – the brain-cognition space – capturing the relationship between brain functions as we know it. The structure of the space allowed us to test the degree of logic in the relationship between functions statistically – a rationality index – and to predict the activation pattern of new and still undetermined functions. The organisation and predictive framework defined by the brain-cognition space will foster the investigation of novel functions and guide the exploration of the fabric of human cognition.

Introduction

Functional neuroimaging has been accumulating a wealth of evidence of the intricate relationship between structure and function. Motor, auditory, and visual functions activations are structurally segregated in the brain. However, activations associated with other cognitive functions might overlap. Working memory[1], spatial attention[23], language[4], and mirror neurons[5] share similar patterns of activation[6]. Hence, the structure of cognitive functions as we know it is not perfectly segregated and challenges our conception of the brain-cognition organisation built on activation models. This is because our representation of cognition has been built on the exploration of theoretical and experimental paradigms that are, in principle, recursively validated. As the quintessence of knowledge is not about absolute truth but knowledge of the art of reasoning itself[7], in order to make progress, our knowledge should always be questioned through rationalisation.

Cognitive neuroscience relies on a changing constellation of ideas on how our mind is ascribed to our brain[8]. Accordingly, mapping brain activations associated with cognition leapt from the one-to-one correlation between brain regions and behaviour to advanced complex neural systems that drive human behaviour[9,10]. However, the exponential increase of task-related functional MRI studies and the avalanche of replication crises hampered the progress of theoretical rationale supporting the cognitive concepts explored[11,12]. Consequently, the potential overlap, independence, granularity of the functions and gap between them remain poorly known at the global level and would require a novel reliable framework.

The recent blossoming of large dataset studies and the introduction of the meta-analytic approach allow for scrutinising the consistency of neuroimaging results[13–17] and reducing the likelihood of false positive errors[18]. The advent of new techniques such as dimensionality embedding allows the visualisation of the complexity inherent in large data by reducing its dimension, allowing probing of the neural cognitive systems as a whole[19,20]. Dimensionality reduction applied to neuroimaging data indicates that a few

embedding components can describe the underlying pattern of functional activation in the brain[21]. Yet, the current spectrum of cognitive domains is limited in its theoretical scaffolding (i.e. epistemology) challenging the establishment of a comprehensive understanding of the brain-cognition organisation[11,12]. Exposing and overcoming the gaps in the current brain-cognition knowledge will require a framework to estimate the degree of logic in the organisation between the functions explored so far – a rationality index. The rationality index, and the underlying structure of our knowledge it represents, will allow new epistemologically unbiased avenues for fMRI exploration.

To extract a latent structure capturing the current brain-cognition knowledge and reveal its rationality we used Neurosynth, the most comprehensive meta-analytic fMRI database (n = 506 meta-analytic maps,[22]), to compute a two-dimensional space embedding -the brain-cognition space (BCS). Each meta-analytic map was parcellated according to the Multi-Modal Parcellation[23], and the AAL3[24,25]. This multi-atlas approach was used to obtain a comprehensive anatomical representation of the maps. The parcellated maps were then embedded using the Uniform Manifold Approximation and Projection method UMAP,[26]). UMAP estimated the similarity between the meta-analytic activation maps and represented it as the euclidean distance between one map and another — thus defining the brain-cognition space (BCS, **Figure 1a**). In other words, BCS represents the relationship between brain functions as we know it. The resulting space had a neuron-like architecture and clustered specific cognitive domains along different branches (e.g. attention, motor, language). Nevertheless, the centre of the space gathered dissimilar cognitive functions (e.g. consciousness, spatio-temporal). The BCS structure incorporates the theoretical and methodological strengths and liabilities of thirty years of fMRI research. Thus, the space properties were leveraged to test the degree of logic in the organisation of functions statistically, measuring the rationality index as the predictability of each functional map from its shared similarities with the others.

To measure the predictability of a map, its euclidean distances from other maps were used as an independent variable and the other meta-analytic maps (n = 505) were included as the dependent variable. The correlations between the measured and the predicted maps (resulting from the 506 regression models) were computed, revealing their level of predictability, or rationality index. The higher the index, the higher the predictability of each map (Figure 1a). Highly predictable maps were mainly located in the neuron branches of the BCS, while its centre was the least predictable. These results indicate that some cognitive functional maps have been less rationally explored with respect to the better-segregated functions. Statistical analysis indicated that the rationality index of functions in the left hemisphere was significantly higher than in the right ($t = 4.2$, $df = 505$, p-value <.001, Figure 1c), indicating that an interhemispheric epistemological imbalance exists in the human brain.

Regression analysis between the measured meta-analytic maps and their rationality index revealed the brain areas that were best predicted. These highly predictable areas included motor, auditory, and primary somatosensory cortices together with the medial temporal (MT) cortex, premotor cortex, frontal and parietal eye fields, supplementary motor area (SMA), caudate, putamen, pallidum, substantia nigra, red

nucleus and basal forebrain in both hemispheres, and 'Broca's area' in the left hemisphere (Figure 2a,b). Accordingly, these areas correspond to brain regions that are the best characterised epistemologically.

The map of the highly characterised structures was compared to the five resting-state gradients that summarise in a data-driven way the brain activations driving human cognition[21]. The results revealed a significant negative correlation with the first and second gradients (rho = -0.3 and rho = -0.48 both with p-values < .001; Figure 2 c,d). This finding indicates that the functionally best-characterised areas correspond to negative values on these two gradients and colocalise mostly with unimodal brain systems with the exception of the SMA, inferior frontal gyrus (Broca territory) and the frontal and parietal eye fields. Accordingly, the characterisation of heteromodal systems would require a more systematic, rational investigation of the already described functions, and the BCS vacant locations -gaps- that are yet to be explored. In order to test whether the BCS can provide a rational framework to fill these gaps we attempted to predict the meta-analytic activation maps of missing (i.e. undetermined) functions. As a proof of concept, unexplored functions located in the aforementioned gaps were validated with out-of-sample maps, including new (delivered by Neurosynth after 2017) meta-analytic activation maps (n = 13; Figure 3a) and recent independent functional MRI work released after 2017 (https://neurovault.org/; n = 19; see Supplementary Material Table 1 for a description of the works; Figure 3b). A total of n=32 new activation maps were projected in the BCS, and they landed on empty locations of the BCS (Supplementary Figure 1). As described before, we statistically compared these new maps with their predictions. Results indicate that new maps landing close to rationally explored functions were reliably predicted, ranging from low to high effect size (0.1< r >0.5).

Discussion

We established a new model of the brain organisation of cognition – the BCS – as derived from the largest meta-analytic database of task-related fMRI. This organisation demonstrated that some functions were better characterised epistemologically, based on their segregation in the BSC, than others, particularly when involving primary cortices (e.g. precentral gyrus, visual cortex). Additionally, the BCS allowed for the prediction of epistemologically unavailable functions that could be validated with recent findings in neuroimaging. Overall, the framework we propose will contribute to a more rational exploration of cognition.

Cognitive domains are clustered within each BCS branch following a neuron-shaped architecture, suggesting a fractal geometry of the relationship between brain structures and functions[27]. The position of the cognitive domains on each branch reflects their mutual relationship within and between branches (see Supplementary Materials for an extensive discussion). For instance, meta-analytic activation maps for reward, learning, and prediction can be found within the decision-making branch. Between branches, the proximity of functions such as emotion and decision-making reflect their close interaction[28]. By contrast, the striking difference in the anatomical pattern of auditory-modality fMRI task necessitates further queries on the possible influence of stimuli modality in activation studies. In fact, the pronounced difference in the auditory cluster could be biased because other cognitive domains are systematically

investigated using, at least partly, visual tasks. Hence, the BCS highlights the strengths and weaknesses in the rationality of cognition as we know it and is a critical step toward its objective improvement.

Some functions are better epistemologically investigated following a gradient distributed from the centre to the periphery of the BCS. This finding exposes the limitations faced by fMRI studies in the past decades. Together with sample size[17,29] and strength of activation[30], the quality of fMRI-designed tasks weighs heavily on the reliability of fMRI activations[31,32]. While previous studies established test-retest reliability of motor, perceptual, and higher-cognition tasks and consistency of the participation of brain structures in specificfunctions[33–36], other experimental tasks poorly replicate[37]. The poor epistemological characterisation of the psychological construct behind the explored cognitive functions and flaws in the experimental design affect the specific targeting of the function of interest[38,39]. The findings of this study reveal the reliably explored functions in 20 years of fMRI literature. We suggest that the low rational index of the maps located in the centre of the space reflects the low epistemological characterisation of their corresponding functions.

In contrast with task-related fMRI, the data-driven decomposition of resting state fMRI can serve as a point of comparison for the epistemological bias. Gradient theory has shown that resting-state brain activation can be summarised according to the main trend of activation of unimodal to higher-cognition regions[21]. Accordingly, our results indicate brain areas that are epistemologically best characterised are mostly located within unimodal systems, with some exceptions for monitoring, language and attentional systems (see Supplementary Materials for an extensive description). Furthermore, comparisons between the left and right hemispheres revealed a rational index asymmetry. Some functions are more lateralised than others (e.g. [40,41]), and our results indicate that the right hemisphere has been less rationally explored and should be prioritised in future cognitive investigations using new tasks.

Such endeavour in the rational exploration of new functions is now feasible since our results demonstrate that new task-related activation maps can be predicted and populate the gaps within and between the BCS branches. Moreover, the prediction of activation maps demonstrates the anatomical fluidity of the transition from one domain to another, suggesting that functions are not strictly segregated but rather fluidly expressed in the brain. Hence, rather than hampering novel explorations, the BCS organisation and predictive framework should be used as an instrument to guide intuitions in exploring the fabric of human cognition built within rational constraints.

Methods

Meta-analytic data thresholding and parcellation

Brain functions were derived from the open-access Neurosynth[22] database, an automated platform that computes whole-brain meta-analytic activation maps for specific cognitive terms. The meta-analytic maps indicate the strength of the activations associated with a specific term as a z-score for each brain voxel. The meta-analytic dataset used in the present study includes 506 functions representative of the

state-of-the-art in the exploration of the anatomy of brain cognition from 1997 to 2017 (11406 literature sources) that were manually curated and validated in a previous study[41]. To allow for the replication of the quantitative relationship between the maps (see Supplementary Materials), only the meta-analytic activation maps that were also available in the 2021 Neurosynth collection were selected. 84 meta-analytic maps missing from the 2021 collection were excluded from the original dataset of[41].

The 506 meta-analytic maps (Neurosynth 2017) were thresholded at z=3.4 (p=0.000337) to ensure the generalisability of the brain-cognition architecture to recent meta-analytic data. Neurosynth applies a threshold of z=3.4 to meta-analytic maps obtained after 2017 to correct for multiple comparisons.

Each map underwent a comprehensive cortical (MMP,[23]) and subcortical (AAL3,[24,25]) parcellation. We thus obtained a total of 440 brain parcels per meta-analytic map and extracted mean z scores for each parcel.

The thresholding and parcellation were applied in FSL (fslmaths and fslstats respectively, https://fsl.fmrib.ox.ac.uk/fsl/fslwiki/FSL).

Brain-cognition space embedding

The Uniform Manifold Approximation and Projection (UMAP,[26]) algorithm was used to reduce the dimensionality of the parcelled meta-analytic dataset in a two-dimensional embedding space.

UMAP is a non-linear low-dimension projection technique that learns the manifold structure of data while retaining its core organisation in a lower dimensionality embedding[26]. UMAP was applied using the eponymous UMAP Python library (umap-learn.readthedocs.io) with default parameters. Specifically, the space was built in two dimensions to foster the interpretability and successive manipulation of the data organisation; the algorithm used the information of 15 local neighbours to learn the manifold structure of the data points; 0.1 minimum distance was allowed by the algorithm to pack the data; the Euclidean metric was used for the data embedding. In the embedding, maps with similar activation patterns clustered together, while different maps spread apart. The Python library Pickle stored the embedded transformation of the meta-analytic dataset as a Python object, allowing the dimensionality reduction and projection of external data in the same embedded space (https://github.com/vale-pak/BCS/tree/BCS_computation).

Rationality index computation

The spatial relationship between meta-analytic activation maps was exploited to test the predictability of the anatomy of each of the functions and obtain a novel index that we will address as a rationality index because it has the property to summarise the embedding space underlying the organisation.

The linear spatial relationship among the maps was computed as the shortest distances (Euclidean distances) between the maps embedded in the BCS. The pattern of activation predicted for each map

was obtained by voxel-wise linear regressions in FSL's (https://fsl.fmrib.ox.ac.uk/fsl/fslwiki/Randomise/UserGuide) randomise where the distances were set as dependent variables, and the 505 maps used to build the BCS (506 - 1 to-be-predicted map) as independent variables. Since the resulting t-stat maps underwent further transformation and thresholding, no permutation was applied to correct for multiple comparisons during the linear regressions. Hence, the 506 t-maps were transformed into z-maps and thresholded at a z=3.4 to allow for the comparison with the measured meta-analytic maps. The rationality index was computed as Pearson's R using fslcc in FSL (https://fsl.fmrib.ox.ac.uk/fsl/fslwiki/Fslutils), comparing each measured meta-analytic map to the corresponding predicted z-map.

Rationality index laterality

The parcels of the 506 predicted maps were divided into left and right hemispheres parcels, and the mean z-statistic of left and right structures was computed for each predicted functional map. Then, the t-test comparison was conducted in JASP (https://jasp-stats.org/) to explore the mean rationality index differences between the left and right hemispheres.

Rationality map computation and correlation with activation gradients

The rationality index computed for each of the 506 meta-analytic maps was used as an independent variable in a linear regression with the measured maps as dependent variables via randomise tool of FSL (https://fsl.fmrib.ox.ac.uk/fsl/fslwiki/FSL/randomise). The regression allowed the identification of structures associated with high rationality index. To test whether the rationality pattern of this map corresponded to a typical gradient activation, Pearson's correlations were computed between the obtained rationality map and each of the five activation gradients[21].

Embedding transformation and prediction of new functions

New, undescribed meta-analytic and raw-data functional activation maps were used for testing the new functions' prediction power of the BCS (https://github.com/vale-pak/BCS/tree/New_maps_projection).

Thirteen new cognitive terms and corresponding meta-analytic maps that were not included in the 2017 dataset were retrieved from the 2021 version of Neurosynth (14371 literature sources). The same exclusion criteria applied for the selection of 2017 maps were used[41]. Briefly, terms referring to studies on neurodevelopmental and brain disorders were not taken into account.

The selection of raw functional activation maps of new studies (i.e. published after 2017) was conducted on Neurovault (https://neurovault.org/). We scrutinised the repository for task-related activation maps of studies published after 2017 using the branches' cognitive domains or the functions with the highest rationality index as keywords. Studies involving psychiatric and pathological populations were not considered. Nineteen new activation maps were selected. When necessary t-stat maps were transformed into z-maps, registered to the MNI152 and thresholded at z=3.4.

All the test data maps (the new meta-analytic and raw activations datasets) underwent the same parcellation as the 2017 maps. Then, UMAP allowed for the two-dimension embedding of the new test data based on the previously defined BCS embedding. Coordinates of the locations of each new map were extracted in the BCS space.

The Euclidean distances between each new map and the 506 BCS-measured maps were exploited as the dependent variable in the linear regressions to predict the anatomy of the new maps. The t-stat maps resulting from the linear regressions were transformed into z-maps, thresholded at z=3.4, and parcellated. The rationality index between the measured and predicted test data were computed using Spearman's correlations.

Declarations

Acknowledgements

The authors would like to thank Dr Gaël Jobart, Dr Marc Joliot and the Groupe d'Imagerie Neurofonctionelle, and Pr Maurizio Corbetta and his team for the inputs and discussions on the study.

This work was supported by the European Union's Horizon 2020 research and innovation programme under the European Research Council (ERC) Consolidator grant agreement No. 818521 (MTdS, DISCONNECTOME), the Marie Skłodowska-Curie grant agreement No. 101028551 (SJF, PERSONALISED), and the Donders Mohrmann Fellowship No. 2401515 (SJF, NEUROVARIABILITY). This work was conducted in the framework of the University of Bordeaux's IdEx "Investments for the Future" program RRI "IMPACT," which received financial support from the French government.

Authors contributions

VP and MTS contributed to the study conceptualization, data curation, formal analysis, investigation, methodology, writing of the original draft, and project administration. VN, LT, and SJF contributed to the study conceptualization, formal analysis, methodology, and writing.

Competing interests

The authors declare no competing interests.

Supplementary materials

Supplementary Information is available for this paper.

Data availability

The dataset and the code used to create and validate the BCS are freely available at https://github.com/vale-pak/BCS.git.

References

1. Cohen, J. D. *et al.* Temporal dynamics of brain activation during a working memory task. *Nat.* **386**, 604–608 (1997).
2. Coull, J. T. & Nobre, A. C. Where and When to Pay Attention: The Neural Systems for Directing Attention to Spatial Locations and to Time Intervals as Revealed by Both PET and fMRI. *J. Neurosci.***18**, 7426–7435 (1998).
3. Corbetta, M. & Shulman, G. L. Control of goal-directed and stimulus-driven attention in the brain. *Nat. Rev. Neurosci.***3**, 201-215 (2002).
4. Price, C. J. A review and synthesis of the first 20 years of PET and fMRI studies of heard speech, spoken language and reading. *Neuroimage***62**, 816–847 (2012).
5. Grèzes, J., Armony, J. L., Rowe, J. & Passingham, R. E. Activations related to “mirror” and “canonical” neurones in the human brain: an fMRI study. *Neuroimage***18**, 928–937 (2003).
6. Parlatini, V. *et al.* Functional segregation and integration within fronto-parietal networks. *Neuroimage***146**, 367–375 (2017).
7. West, T. G. *Plato’s Apology of Socrates. An Interpretation, with a New Translation*. (Cornell University Press, 1980).
8. Thiebaut de Schotten, M. & Forkel, S. J. The emergent properties of the connected brain. *Science***378**, 505–510 (2022).
9. Friston, K. J. Models of brain function in neuroimaging. *Annu. Rev. Psychol.***56**, 57–87 (2005).
10. Nozais, V., Forkel, S. J., Foulon, C., Petit, L. & Thiebaut de Schotten, M. Functionnectome as a framework to analyse the contribution of brain circuits to fMRI. *Commun. Biol.***4**, (2021).
11. Pessoa, L., Medina, L. & Desfilis, E. Refocusing neuroscience: moving away from mental categories and towards complex behaviours. *Philos. Trans. R. Soc. B***377**, 20200534 (2022).
12. Box-Steffensmeier, J. M. *et al.* The future of human behaviour research. *Nat. Hum. Behav.***6**, 15–24 (2022).
13. Derrfuss, J. & Mar, R. A. Lost in localization: the need for a universal coordinate database. *Neuroimage***48**, 1–7 (2009).
14. Eickhoff, S. B. *et al.* Coordinate-based activation likelihood estimation meta-analysis of neuroimaging data: a random-effects approach based on empirical estimates of spatial uncertainty. *Hum. Brain Mapp.***30**, 2907–2926 (2009).
15. Pinho, A. L. *et al.* Individual Brain Charting, a high-resolution fMRI dataset for cognitive mapping. *Sci. Data 2018 51***5**, 1–15 (2018).
16. Swick, D. & Chatham, C. H. Ten years of inhibition revisited. *Neuroscience***8**, 1–2 (2014).
17. Marek, S. *et al.* Reproducible brain-wide association studies require thousands of individuals. *Nature* **603**, 654–660 (2022).

18. Radua, J. & Mataix-Cols, D. Meta-analytic methods for neuroimaging data explained. *Biol. Mood Anxiety Disord.***2**, 2-6 (2012).
19. Beam, E., Potts, C., Poldrack, R. A. & Etkin, A. A data-driven framework for mapping domains of human neurobiology. *Nat. Neurosci.***24**, 1733-1744 (2021).
20. Talozzi, L. *et al.* Latent disconnectome prediction of long-term cognitive symptoms in stroke. Preprint at https://www.researchsquare.com/article/rs-1181593/v1 (2021)
21. Margulies, D. S. *et al.* Situating the default-mode network along a principal gradient of macroscale cortical organization. *Proc. Natl. Acad. Sci. U. S. A.***113**, 12574–12579 (2016).
22. Yarkoni, T., Poldrack, R. A., Nichols, T. E., Van Essen, D. C. & Wager, T. D. Large-scale automated synthesis of human functional neuroimaging data. *Nat. Methods***8**, 665-670 (2011).
23. Glasser, M. F. *et al.* A multi-modal parcellation of human cerebral cortex. *Nature***536**, 171-178 (2016).
24. Rolls, E. T., Huang, C. C., Lin, C. P., Feng, J. & Joliot, M. Automated anatomical labelling atlas 3. *Neuroimage***206**, 116-189 (2020).
25. Huang, C. C., Rolls, E. T., Feng, J. & Lin, C. P. An extended Human Connectome Project multimodal parcellation atlas of the human cortex and subcortical areas. *Brain Struct. Funct.***227**, 763-778 (2022).
26. McInnes, L., Healy, J., Saul, N. & Großberger, L. UMAP: Uniform Manifold Approximation and Projection. Preprint at https://arxiv.org/abs/1802.03426 (2018).
27. Mandelbrot, B. B. *The Fractal Geometry of Nature*. (Freeman Press, 1982).
28. Bechara, A., Damasio, H. & Damasio, A. R. Emotion, Decision Making and the Orbitofrontal Cortex. *Cereb. Cortex***10**, 295–307 (2000).
29. Turner, B. O., Paul, E. J., Miller, M. B. & Barbey, A. K. Small sample sizes reduce the replicability of task-based fMRI studies. *Commun. Biol.***1**, (2018).
30. Kampa, M. *et al.* Replication of fMRI group activations in the neuroimaging battery for the Mainz Resilience Project (MARP). *Neuroimage***204**, 116223 (2020).
31. Plichta, M. M. *et al.* Test-retest reliability of evoked BOLD signals from a cognitive-emotive fMRI test battery. *Neuroimage***60**, 1746–1758 (2012).
32. Bennett, C. M. & Miller, M. B. FMRI reliability: Influences of task and experimental design. *Cogn. Affect. Behav. Neurosci.***13**, 690–702 (2013)
33. Yoo, S. S., Wei, X., Dickey, C. C., Guttmann, C. R. G. & Panych, L. P. Long-Term Reproducibility Analysis of fMRI using Hand Motor Task. *Int. J. Neurosci.* **115**, 55–77 (2009).
34. Kiehl, K. A. & Liddle, P. F. Reproducibility of the hemodynamic response to auditory oddball stimuli: A six-week test–retest study. *Hum. Brain Mapp.***18**, 42–52 (2003).
35. Aron, A. R., Gluck, M. A. & Poldrack, R. A. Long-term test-retest reliability of functional MRI in a classification learning task. *Neuroimage***29**, 1000–1006 (2006).
36. Johnstone, T. *et al.* Stability of amygdala BOLD response to fearful faces over multiple scan sessions. *Neuroimage***25**, 1112–1123 (2005).

37. Bennett, C. M. & Miller, M. B. How reliable are the results from functional magnetic resonance imaging? *Ann. N. Y. Acad. Sci.***1191**, 133–155 (2010).
38. Poldrack, R. A. The future of fMRI in Cognitive Neuroscience. *Neuroimage***62**, 1216-1220 (2012).
39. Hay, L., Duffy, A. H. B., Gilbert, S. J. & Grealy, M. A. Functional magnetic resonance imaging (fMRI) in design studies: Methodological considerations, challenges, and recommendations. *Des. Stud.***78**, 101078 (2022).
40. Ambrosini, E., Arbula, S., Rossato, C., Pacella, V. & Vallesi, A. Neuro-cognitive architecture of executive functions: A latent variable analysis. *Cortex***119**, 441–456 (2019).
41. Karolis, V. R., Corbetta, M. & Thiebaut de Schotten, M. The architecture of functional lateralisation and its relationship to callosal connectivity in the human brain. *Nat. Commun.***10**, 1417 (2019).

Figures

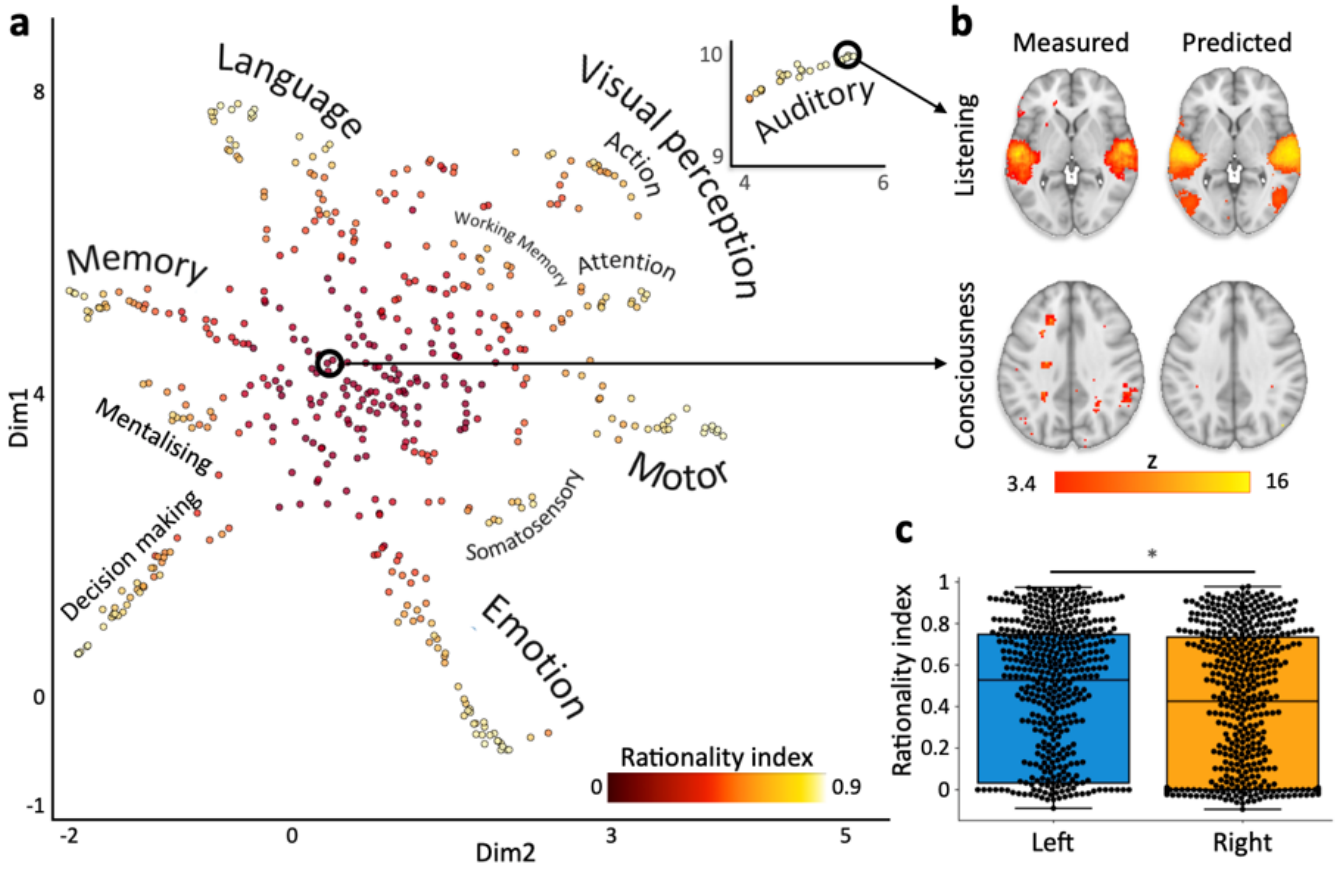

Figure 1

The Brain-Cognition Space (BCS) and the rationality index. a) In the BCS, similar functional meta-analytic maps cluster together. The colour bar indicates the rationality index (i.e. the degree of logic in the

organisation between functions). Corresponding cognitive domains are indicated next to each branch. b) Representative examples of the best (listening) and worst (consciousness) measured (left) and predicted (right) pair of meta-analytic maps. The colour bar represents the z-statistic of voxels from the Neurosynth meta-analysis maps (measured) and voxels resulting from the voxel-wise linear regression (predicted). c) The difference between the mean rationality index of the left (blue) and right (orange) hemispheres. *, p < 0.001. Lines, boxes, whiskers and dots represent the median, quartiles, distribution, and observations.

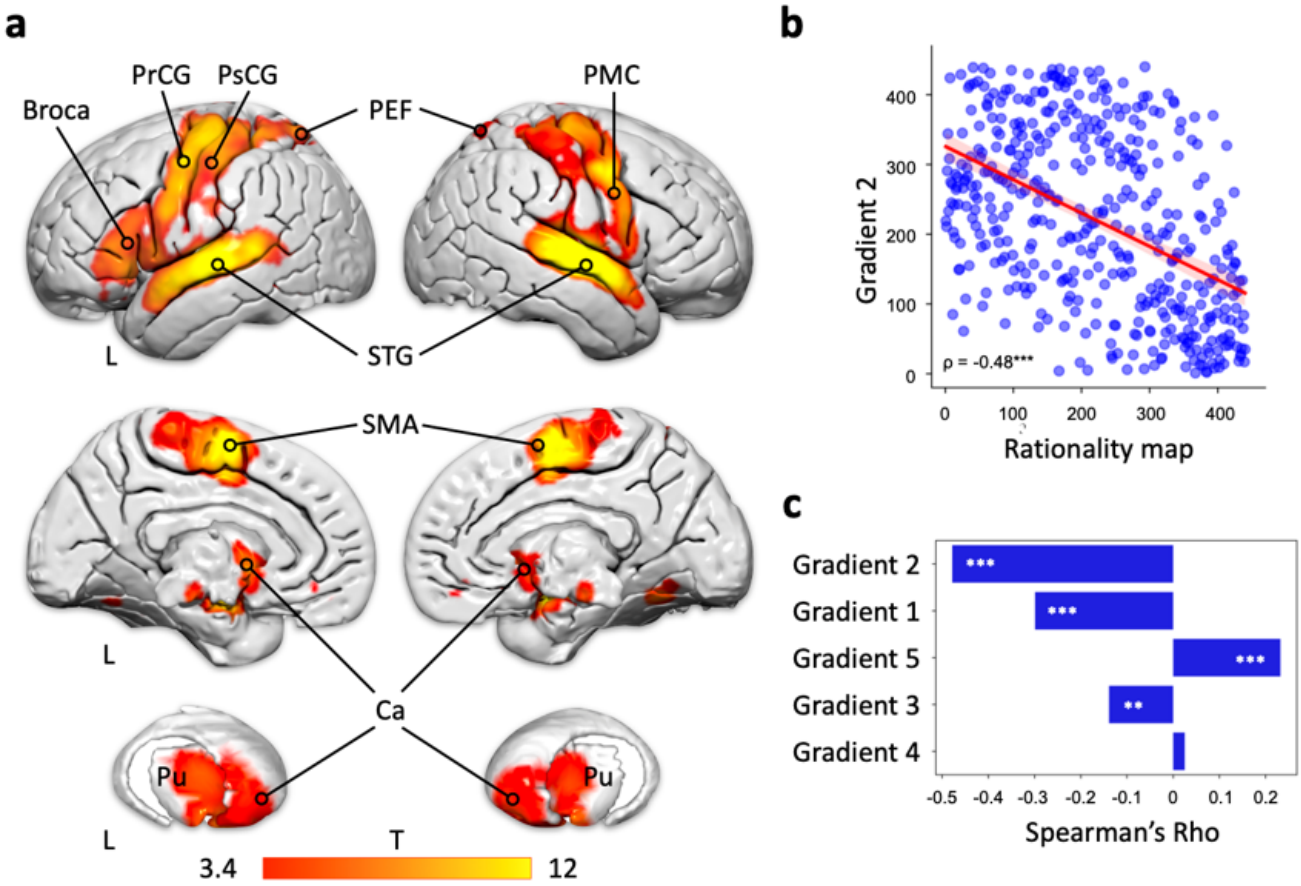

Figure 2

Epistemologically best-characterised areas and their relationship with the data-driven domain-wise organisation of brain functions (i.e. resting-state fMRI gradients). a) Left and right lateral (top), left and right medial (bottom) views and 3D reconstruction of and coronal view of the brain structures that are the best characterised functionally (rationality map). b) Rank scatter plot of the strongest correlation between the rationality map and the second gradient. The regression line is shown in red. c) Spearman correlation between the rationality map and the five resting-state fMRI gradients. *** = p < .001, ** = p < .01. Broca: Broca's area. Ca: caudate nucleus. PEF: parietal eye field. PMC: premotor cortex. PrCG: precentral gyrus. PsCG: postcentarl gyrus. Pu: putamen.

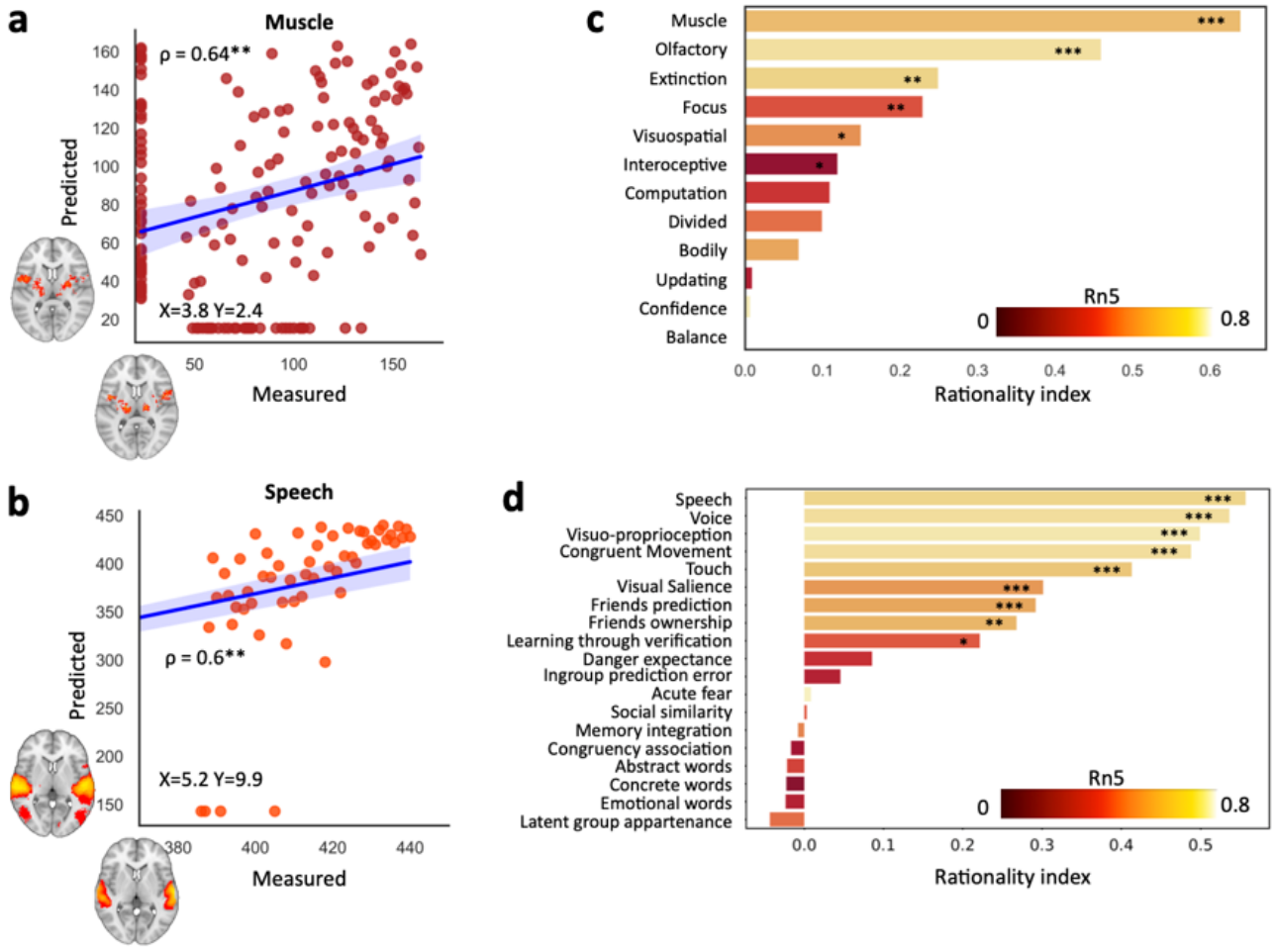

Figure 3

Prediction of unexplored functions with the BCS. Example of Spearman rank correlation between the predicted activations and the later (after 2017) reported (a) meta-analytic and (b) independent fMRI maps. Bar plots indicate the rationality index for (c) meta-analytic and (d) independent fMRI maps. For each new map, bar colours indicate the rationality index of their five nearest neighbours in the BCS (Rn5). *** = p < .001, ** = p < .01, * = p < .05. ρ: spearman's rho. X and Y coordinates represent each measured map's location in the space (see supplementary Figure 1 for a visual representation).

Supplementary Files

This is a list of supplementary files associated with this preprint. Click to download.

- SupplementaryInformationPacellaetal2022.docx